Improving the blind restoration of retinal images by means of point-spread-function estimation assessment

Andrés G. Marrugo[a], María S. Millán[b], Michal Šorel[c], Jan Kotera[c], and Filip Šroubek[c]

[a]Facultad de Ingeniería, Universidad Tecnológica de Bolívar
Km 1 vía Turbaco, Cartagena, Colombia.

[b]Department of Optics and Optometry, Universitat Politècnica de Catalunya
Violinista Vellsolà 37, 08222 Terrassa, Spain.

[c] Institute of Information Theory and Automation, Academy of Sciences
Pod Vodárenskou věží 4, 18208 Prague 8, Czech Republic.

ABSTRACT

Retinal images often suffer from blurring which hinders disease diagnosis and progression assessment. The restoration of the images is carried out by means of blind deconvolution, but the success of the restoration depends on the correct estimation of the point-spread-function (PSF) that blurred the image. The restoration can be space-invariant or space-variant. Because a retinal image has regions without texture or sharp edges, the blind PSF estimation may fail. In this paper we propose a strategy for the correct assessment of PSF estimation in retinal images for restoration by means of space-invariant or space-invariant blind deconvolution. Our method is based on a decomposition in Zernike coefficients of the estimated PSFs to identify valid PSFs. This significantly improves the quality of the image restoration revealed by the increased visibility of small details like small blood vessels and by the lack of restoration artifacts.

Keywords: Medical image, retinal image, deconvolution, deblurring, point-spread-function.

1. INTRODUCTION

Blur is one of main image quality degradations in eye fundus imaging which hinders the clinical use of the images. Its main causes are: inherent optical aberrations in the eye, relative camera-eye motion, and improper focusing. Because the optics of the eye is part of the optical imaging system, eye aberrations are a common source of image degradation. The technique for recovering an original or unblurred image from a single or a set of blurred images in the presence of a poorly determined or unknown *point spread function* (PSF) is called *blind deconvolution*. For the restoration of retinal images, we have proposed[1] a blind deconvolution method to restore blurred retinal images acquired several months apart, even when structural changes had occurred in the retina. However, the method is limited to images blurred uniformly; in other words, we assumed the blur to be space-invariant.

For the case when the blur varies across the field of view we proposed a space-variant (SV) approach.[2,3] To carry out the restoration, we assume that in small regions the space-variant blur can be approximated by a space-invariant PSF. However, instead of deblurring the image on a per-patch basis, we extend individual PSFs by linear interpolation and perform a global restoration. Despite our efforts in building a robust blind deconvolution method, the blind estimation either of a space-invariant or space-variant PSF may fail which significantly hinders the quality of the image restoration. The purpose of this work is to illustrate the problem of PSF estimation failure in retinal images and to develop a method for the correct identification of the most accurate PSFs. This should enable better restoration results using the same deconvolution procedure reported in Refs. 1, 2.

It has been shown that in image deblurring, first estimating the PSF and then solving a non-blind deconvolution problem with the estimated PSF produces adequate results.[4] In this situation, the quality of the restoration

Further author information: (Send correspondence to A.G. Marrugo)
A.G.M.: E-mail: agmarrugo@utbvirtual.edu.co, Telephone: +57 5 6535200 - 306.

10th International Symposium on Medical Information Processing and Analysis,
edited by Eduardo Romero, Natasha Lepore, Proc. of SPIE Vol. 9287, 92871D
 · doi: 10.1117/12.2073820

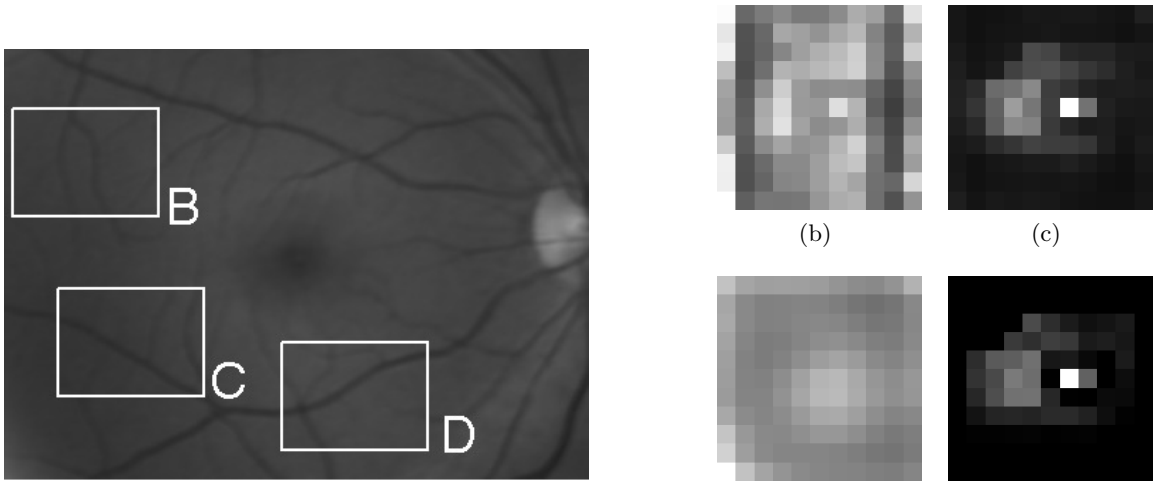

(a) (b) (c) (d) (e)

Figure 1. a) Retinal image artificially degraded. (b)-(d) Estimated PSFs from three different regions. (e) Original PSF. Notice that not all estimated PSFs are similar to the original.

is directly affected by the performance of the PSF estimation. That is, the image can be restored successfully if the PSF can be accurately estimated. In Fig. 1 we show an example of different PSFs estimated from different regions of the retinal image. Several estimated PSFs differ significantly from the original PSF shown in Fig. 1(b). Typically recovering the PSF from the whole image is not optimal and more computationally demanding. However, in the case of SV blur the SV PSF needs to be recovered from several regions of the image despite the fact that not all regions may prove suitable for successful PSF recovery.

2. METHOD

In this paper we use a multichannel deconvolution approach[1,5,6] to estimate the PSFs from a pair of degraded retinal images. We use the PSF similarity S measure from Hu and Yang[7] to compare the estimated PSF with the ground-truth. The authors showed in the paper that this measure is more accurate than the root mean square error, especially because it is shift invariant. The measure is defined as the blur kernel similarity $S(h, \tilde{h})$ of two kernels, h and $\tilde{h}$,

$$S(h, \tilde{h}) = \max_{\gamma} \rho(h, \tilde{h}, \gamma) \ , \tag{1}$$

where $\rho(.)$ is the normalized cross-correlation function and γ is the possible shift between the two kernels. Let τ represent element coordinates, $\rho(.)$ is given by

$$\rho(h_p, \tilde{h}_p, \gamma) = \frac{\sum_{\tau} h_p(\tau) \cdot \tilde{h}_p(\tau + \gamma)}{\|h_p\| \cdot \|\tilde{h}_p\|} \ , \tag{2}$$

where $\|\cdot\|$ is the ℓ_2-norm. Larger similarity values reflect more accurate PSF estimation, thus better image restoration. The authors showed that the similarity measure is spatially correlated with the MSE estimated by restoring the blurred image and comparing with the original image. While this approach works sufficiently well on motion blur, in this paper we show that it doesn't work well with blur arising from optical aberrations or similar image degradations.

In Fig. 1 we show an example of a degraded retinal image and in Fig. 2(a) the computed PSF similarity map for this image. Notice that not from all regions are PSFs accurately estimated. For restoring retinal images by means of blind deconvolution it has been suggested that the sub-window for PSF estimation has to be placed on top of retinal structures, like blood vessels. However, as we see in Fig. 2(a), this is not always the case. In the following we explore the question of how to reliably estimate accurate PSFs.

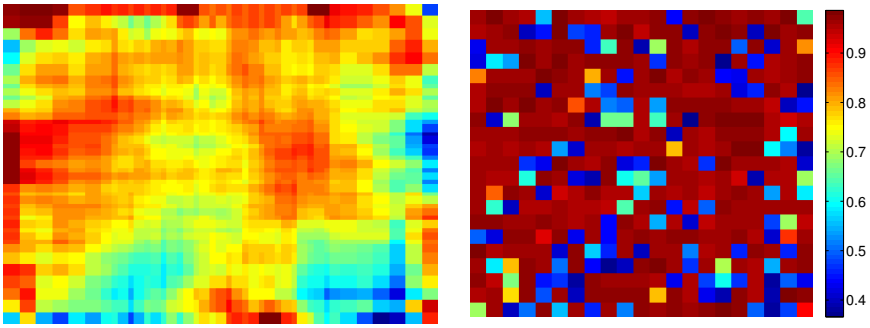

(a) (b)

Figure 2. (a) PSF similarity map. (b) PSF similarity values per sub-window (blue to red pixels indicate low to high PSF similarity compared with the ground truth kernel).

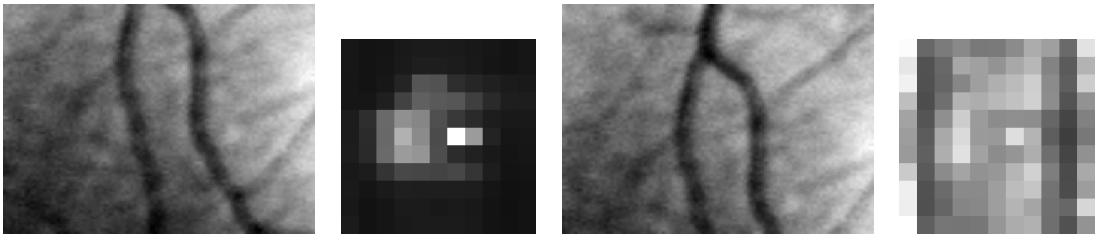

(a) (b) (c) (d)

Figure 3. Two nearby sub-windows (a) and (c) with similar structures, but different estimated PSFs (b) and (d), respectively. The PSF similarity values for (b) $S = 0.962$ and (d) $S = 0.419$. The original PSF is shown in Fig. 1(e).

2.1 Reliable PSF estimation

As described in several papers, edges found in the original blurry image are particularly useful for estimating the PSF. However, as we see from Fig. 1 this may not be entirely true for retinal images. In fact, the spatial correlation between the PSF similarity map and the edge distribution in the retinal image is low. The PSF similarity map was described by Hu and Yang[7] to demonstrate that the high kernel similarity values match low image reconstruction errors. Nonetheless, their approach is based on the assumption that two closely overlapping sub-windows (e.g. shifted a few pixels in either directions) share similar structures. Along the same line, it is reasonable to expect that other sub-windows, nearby a potential good sub-window for kernel estimation, contain useful image structures for deblurring. The deblurred results for these sub-windows should be similar. In this paper, we have found that for this purpose, the PSF similarity map can indeed be misleading. In Fig. 2(b) we show the PSF similarity values per sub-window for the image shown in Fig. 1(a). Note how low similarity values (blue) are distributed uniformly throughout the image alternating with high values (red). Moreover, there are hardly any smooth transitions between high and low similarity values. This alternating characteristic is lost when computing average values per pixel from the sub-windows to build the PSF similarity map. To further illustrate this problem, in Fig. 3 we show two nearby sub-windows from the retinal image from Fig. 1. Because these sub-windows are very similar, we expect the PSF estimation to produce similar results, but the PSF similarity values differ significantly.

The optics of the eye is part of the imaging system, therefore it is reasonable to assume that the PSF os the imaging system is strongly determined by the PSF of the eye. The retinal camera can be close to diffraction limited with a very narrow PSF, but the optics of the eye is governed by optical aberrations.[8] Optical aberrartions are typically described using Zernike polynomials, which can then be related to refraction errors.

As we have seen, PSF estimation in retinal images is not entirely reliable in terms of accurate PSF recovery throughout the field of view. To overcome this limitation, in this paper we propose to characterize the estimated PSFs from the degraded retinal image using Zernike polynomials. On the one hand, an accurately estimated PSF should show high coefficients for typical refraction errors, like defocus (4th coefficient), astigmatism (5th

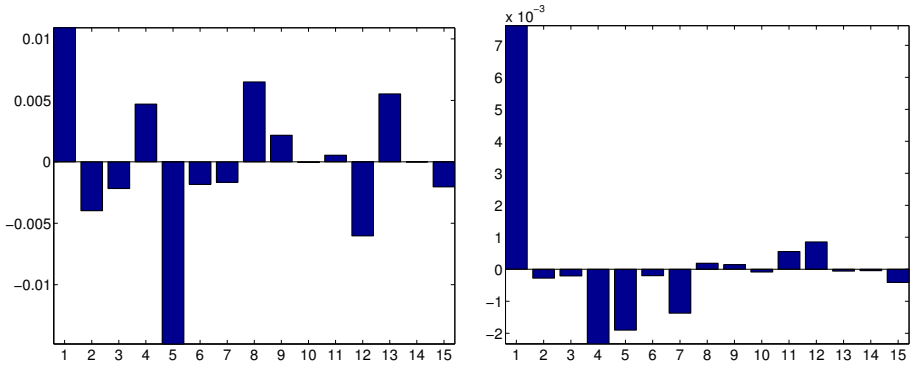

(a) (b)

Figure 4. The first 15 Zernike coefficients for the PSFs shown in (a) Fig. 3(b) and (b) Fig. 3(d).

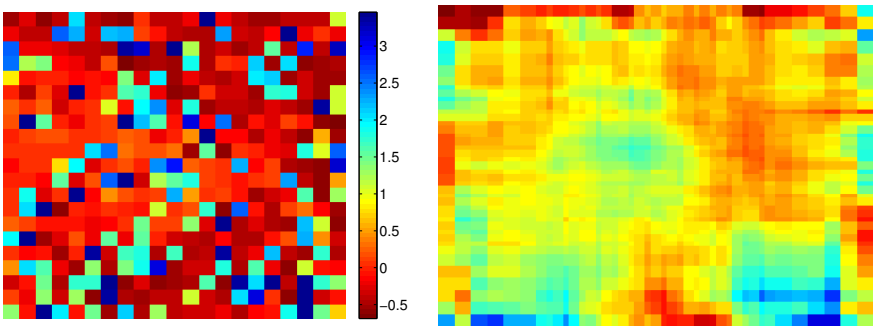

(a) (b)

Figure 5. (a) Zernike coefficients skewness values per sub-window.(b) Zernike coefficients skewness map (blue to red pixels indicate positive to negative skewness). This correlates well with the PSF similarity map shown in Fig. 2.

and 6th coefficients), coma (7th and 8th coefficients). On the other hand, we consider that a PSF that does not follow this general pattern is not valid and most likely corresponds to a failed estimation.

In order to prove this, we designed an artificial experiment where we compare the estimated PSFs with the ground-truth PSF using the kernel similarity measure S. In Fig. 4 we show the Zernike coefficients for the two PSFs shown in figures 3(b) and 3(d). Notice how the highest coefficient from Fig. 4(a) is the 5th which is related to *astigmatism*. In contrast, the highest coefficient for the PSF in in Fig. 4(b) is the 1st, which is called *piston*. The piston equals to the mean value of the wavefront. It is not actually a *true* optical aberration, as it does not represent or model curvature in the wavefront. In fact, defocus is the lowest-order true optical aberration.

To characterize this difference, and thus identify PSF estimation failure we carry out the following. Let us consider the Zernike coefficients as a probability distribution and compute the skewness of the distribution as a measure of symmetry. The skewness γ_1 of a random variable X is defined as

$$\gamma_1 = E\left[\frac{X-\mu}{\sigma}\right] \quad , \tag{3}$$

where μ and σ are the mean and standard deviation, respectively. The skewness value can be positive or negative. A positive skew indicates that the tail on the right side is longer than the left side, we use this as an indication of PSF estimation failure.

In Fig. 5 we show the skewness values for the estimated PSFs for all sub-windows. Notice that blue squares (positive skewness) are considered failed PSF estimations. Compare with Fig. 2, the distribution is similar. If we compute a Zernike coefficients skewness map for all pixels of the image, we get a distribution that resembles the PSF similarity map from Fig. 2(a).

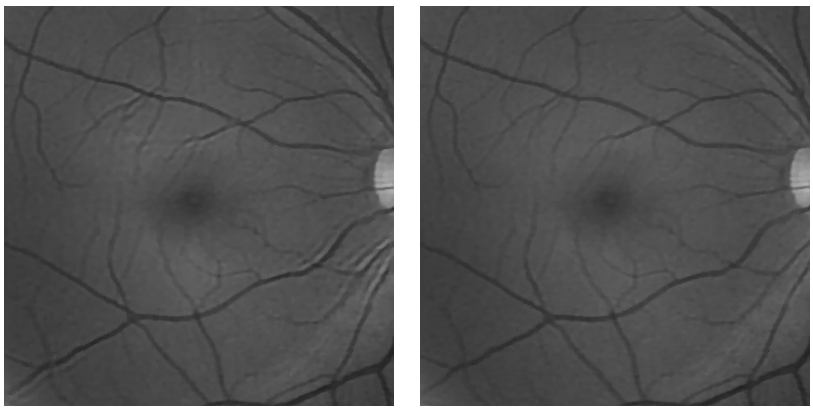

(a) (b)

Figure 6. (a) Restoration with direct estimated PSFs (notice the artifacts due to PSF estimation failure) and (b) restoration by leaving out non-valid PSFs.

In order to use the skewness of the Zernike coefficients as a descriptor for identifying accurately estimated PSFs we carry out the following. We set the value of 0.8 as the threshold for the PSF similarity measure, i.e. all estimated PSFs with $S \geq 0.8$ are considered valid PSFs that lead to a successful restoration. To classify the skewness of the Zernike coefficients for the estimated PSFs as valid or non-valid PSFs we use Otsu's method[9] as clustering technique. It calculates the optimum threshold separating the two classes so that their combined intra-class variance is minimal. More advanced clustering techniques can be used, but because the skewness resulted in high spatial correlation with the PSF similarity measure the chosen method is sufficient. For the PSF similarity values shown in Fig. 2 we have the following values. A total of 441 PSFs were estimated on 21×21 sub-windows. 313 PSFs estimated resulted in PSF similarity values of 0.8 or greater. Using the skewness we were able to predict 333 PSFs as valid. This results in a true positive rate of 0.94%. The important aspect of this approach is that we are interested in determining the most accurately estimated PSFs to obtain the best restoration possible. In addition, because we carry out this approach throughout the whole image it serves both the space-invariant and the space-variant deconvolution methods.

3. RESULTS

In Fig. 6(a) we show the restored artificial image with a randomly chosen estimated PSF. The effect of a non-valid PSF is evident in the poor quality of the restoration and the ringing artifacts. In Fig. 6(b) we show the restoration by selecting the estimated PSF with the proposed method. The restoration improves significantly. In Fig. 7 we show a the restoration of a real degraded retinal image. In Fig. 7(b) we show the space-variant restoration with direct estimated PSFs. The ringing artifacts are evident which are evidence of PSF estimation failure. In contrast, in Fig. 7(c) we show the restoration by leaving out the non-valid PSFs shown in Fig. 8.

4. CONCLUSIONS

Prior to deconvolution the PSF estimation may fail which hinders the restoration procedure. To overcome this limitation we developed a PSF estimation assessment strategy based on the Zernike coefficients of the estimated PSFs to identify valid PSFs. With the artificial experiment we showed how our approach significantly improves the identification of valid PSFs, thus leading to a better restoration. The results on naturally degraded images validate our apporach with notable enhancement throughout the whole image.

REFERENCES

[1] Marrugo, A. G., Sorel, M., Sroubek, F., and Millán, M. S., "Retinal image restoration by means of blind deconvolution," *Journal of Biomedical Optics* **16**(11), 116016 (2011).

[2] Marrugo, A. G., Millán, M. S., Šorel, M., and Šroubek, F., "Restoration of retinal images with space-variant blur," *Journal of biomedical optics* **19**(1), 016023–016023 (2014).

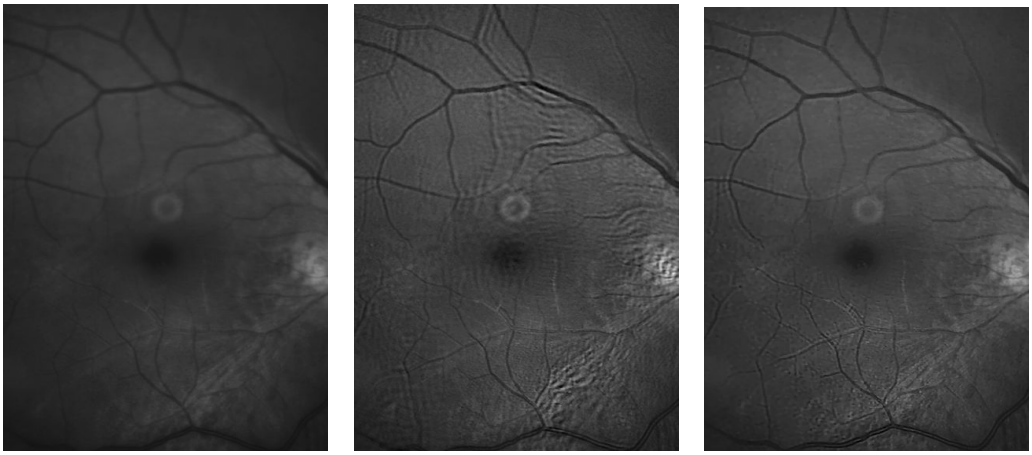

(a) (b) (c)

Figure 7. (a) Real degraded image, (b) space-variant restoration with direct estimated PSFs, and (c) space-variant restoration with valid PSFs.

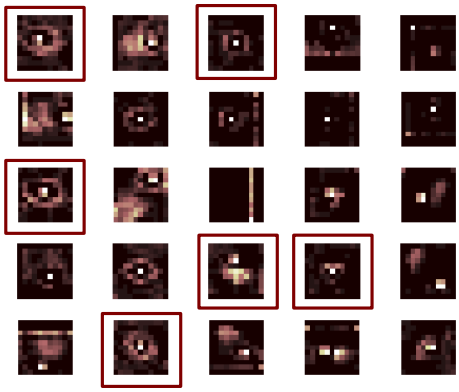

Figure 8. PSF grid estimated for the real degraded retinal image. The PSFs within red squares correspond to the valid PSFs.

[3] Marrugo, A. G., Millan, M. S., Sorel, M., and Sroubek, F., "Blind restoration of retinal images degraded by space-variant blur with adaptive blur estimation," in [*8th Ibero American Optics Meeting/11th Latin American Meeting on Optics, Lasers, and Applications*], Martins Costa, M. F. P. C., ed., 8785D1, SPIE (Nov. 2013).

[4] Levin, A., Weiss, Y., Durand, F., and Freeman, W., "Understanding Blind Deconvolution Algorithms," *Pattern Analysis and Machine Intelligence, IEEE Transactions on* **33**(12), 2354–2367 (2011).

[5] Sroubek, F. and Flusser, J., "Multichannel blind deconvolution of spatially misaligned images," *IEEE transactions on image processing : a publication of the IEEE Signal Processing Society* **14**, 874–883 (July 2005).

[6] Sroubek, F. and Milanfar, P., "Robust Multichannel Blind Deconvolution via Fast Alternating Minimization," *Image Processing, IEEE Transactions on* **21**(4), 1687–1700 (2012).

[7] Hu, Z. and Yang, M.-H., "Good regions to deblur," in [*Computer Vision–ECCV 2012*], 59–72, Springer (2012).

[8] Navarro, R., "The Optical Design of the Human Eye: a Critical Review," *J Optom* **2**, 3–18 (2009).

[9] Otsu, N., "A Threshold Selection Method from Gray-Level Histograms," *Systems, Man and Cybernetics, IEEE Transactions on* **9**(1), 62–66 (1979).